

Multi-Objective Prediction of Drilling EMS-45 with Finite Element, Backpropagation Neural Network, and Metaheuristic Model

M.K. Effendi^{1*}, A.S. Pramono¹, Suhardjono¹, Sampurno¹, D. Harnany¹, F.D. Pratiwi²

¹Department of Mechanical Engineering, ITS, Sukolilo Surabaya 60111, Indonesia

²Department of Mechanical Engineering, ITS, Universitas Muhammadiyah Magelang Jl.Mayjend Bambang Soegeng KM.5 Mertoyudan Magelang 56172

Received: 9 November 2023, Revised: 25 February 2024, Accepted: 25 February 2024

Abstract

Making holes with the minimum thrust force and torque using a drilling machine is challenging for researchers because of the difficulties in setting input parameters such as the type of drill tool, point of angle, and feeding speed. Therefore, the trial-and-error method to predict optimum input parameters through experiment can be replaced with the Back Propagation Neural Network (BPNN) and metaheuristic method (i.e., genetic algorithm (GA) and Simulated Annealing (SA)) method to reduce costs and time. BPNN can be used to represent the input-output correlation precisely. However, obtaining a model with minimum Mean Squared Error (MSE) requires much data for training, testing, and validation. Since the obtained data from experiments requires expensive costs, combining data from experimental and simulation using ANSYS should be considered to reduce the experimental costs. This study was then conducted to answer the research problem using an EMS 45 tool steel as the workpiece, with the three input parameters: type of drill tools (HSS M2 and HSS M35), the points of angle (118 and 134 degrees) and feeding speed rates (0.07 and 0.1 mm/s). The 32 data from experimental and modeling were used to model the correlation between the input and output parameters of the drilling process using BPNN. The BPNN's network model with minimum MSE is then used as the objective function to determine the input parameters to obtain the smallest value of thrust force and torque using the hybrid method using GA and SA. As the results, the optimum output parameter value in drilling for material EMS-45 (i.e., thrust force = 1615.2 N, and torque = 3.0236 Nm) can be obtained with the following input specifications: (a) type of drill tool = HSS-M2, (b) point of angle = 132.28°, (c) feeding speed = 0.1 mm/s.

Keywords: Drilling, Finite Element Method (FEM), Backpropagation Neural Network (BPNN), Genetic Algorithm (GA), Simulated Annealing (SA)

1. Introduction

Determining the correlation of input and response parameters in manufacturing processes is essential for modern automated industries to achieve a high level of effectiveness, efficiency, and economic competitiveness. The important role of the finite element method (FEM) in the manufacturing process has been recognized for its contribution to accurately predict the relationship between input and output parameters in a manufacturing process. Meanwhile, the implementation method is considered to be highly beneficial for the manufacturing industry to reduce the experimental and manufacturing costs, while increasing the economic value of a product [1–3].

In essence, there have been numerous studies that applied FEM to analyze different input parameters on out-

put parameters in drilling. One of them was by Singh, et al. [4] was modeled the effect of input drilling parameters (point of angle, speed, and feed) with output parameters (thrust force and torque) for Fiber Reinforced Plastics (FRP) materials using FEM. A statistical method of ANOVA was then used to predict the level of damage to the drilling tools. Next, Strenkowski et al. [5] determined the minimum value of thrust force and torque in a drilling process using Eulerian finite element. The input drilling parameters observed consisted of spindle speed and feed rate, and the material used in the experiment was AISI 1020. Meanwhile, some authors used a 3D model of FEM to investigate the effect of speed and feed rate on the value of thrust force, torque, and delamination in the drilling process for composite materials, titanium alloys, and bones [6–9].

*Corresponding author. Email: khoirul_effendi@me.its.ac.id.

© 2024. The Authors. Published by LPPM ITS.

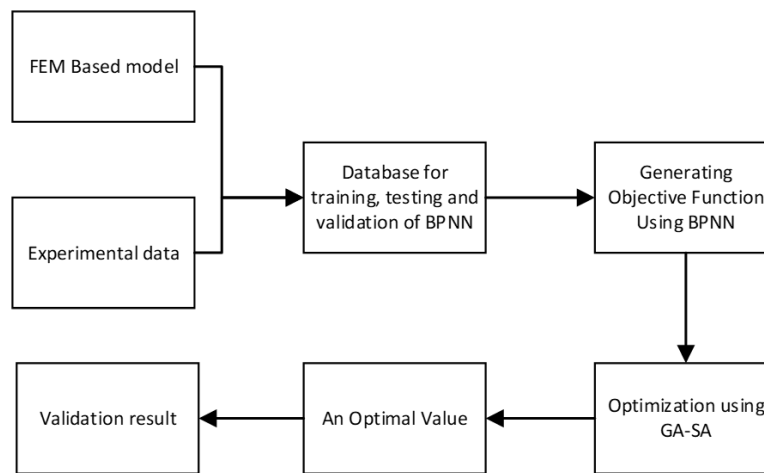


Figure 1. General flowchart of research

Further, the utilization of artificial intelligence (AI) using a backpropagation neural network (BPNN) has become an increasingly popular method for modeling the correlation between input and output parameters of the manufacturing process, such as milling and drilling. Nurullah et al. [10] and Ighravwe et al. [11] utilized the combination of BPNN and optimization methods to obtain minimum surface roughness on milling. Furthermore, Panda et al. [12] and Singh et al. [13] used BPNN for wear monitoring on drill tool tips. Panda et al. [14] used a combination of BPNN and radial basis function network (RBFN) to predict flank wear on a drilling tool. Then, Soepangkat et al. [15] used BPNN-PSO to investigate the effect of drill bit geometry, spindle speed, and feeding speed in drilling for CFRP materials. The results of the BPNN modeling were later used to determine parameters for the minimum delamination using the PSO method.

Sonkar et al. [16] used Taguchi and ANOVA methods to solve a multi-objective optimization problem of a drilling process on a glass fiber-reinforced polymer (GFRP) material. This study aimed to minimize the value of drill force, torque, and delamination as well as improve the quality of surface roughness by selecting the appropriate drilling input parameters (drill speed, feed rate, drill diameter, and plate thickness).

By considering the importance of FEM, AI, and optimization methods in predicting drilling output parameters, we determine to combine these three methods for this research. The drilling input parameters include the type of tool (HSS M2 and HSS M35 variations), points of angle (118 and 134 degrees), and feeding speed (0.07 and 0.1 mm/s), and the output parameters to be studied are thrust force and torque. The output optimization is predicted using a combination of BPNN, GA, and SA methods. The general flowchart of this research can be seen in Fig. 1.

In regards to AI, if we increase the data number on the training, testing, and validation process, then the predictions generated by AI will be more accurate. Therefore, FEM is a low-cost alternative method to reproduce addi-

tional data in this case. This data will later be used to increase the existing data obtained from the experimental step.

In implementing FEM, the first step is to define theoretical assumptions in the 3D FEM simulation. Supposedly, the difference between the results of modeling using finite element and experimental methods remains above 10%, hence a feedback process is carried out to update the parameter settings in the FEM modeling. However, when the error value is already below 10%, the modeling results can directly be used to obtain the data for the drilling process.

All experimental and modeling data are divided into three, namely training, testing, and validation processes. The three data groups are used to model the relationship between input and output parameters in the drilling process using BPNN. Later, the model that BPNN has generated is used as an objective function. Next, GA and SA methods are applied to this function to obtain the optimal value.

GA and SA are two common metaheuristic methods used in solving multi-objective cases. GA can perform a non-linear case optimization process and run a systematic random search to achieve the optimal global value [17, 18]. Although it has several advantages, this method can be trapped in the optimal local area and take a long time to get to the optimal solution [19]. Meanwhile, the SA method can quickly produce the local optimum value. Nevertheless, this method is considered to be weak in achieving the global optimum [20, 21]. Therefore, a combination of GA and SA is expected to minimize the weaknesses and keep the advantages so that the combination method can produce the optimal solution in the shortest time possible. In the first step, the GA is used to identify an initial solution. This initial solution is then used as an input for the SA to identify a global optimum. The combination of the methods is later used to predict the most appropriate combination of input parameters. By then, the drilling process can be done with the smallest possible value of thrust force and torque.

Table 1. Properties of drilling tool

Material	HSS-M2 and HSS-M35
Diameter	10 mm
Length of drill bit	134 mm
Total Flute	2
Producer	Sunflower
Min-max RPM	1500 – 2500 RPM
Point angle	118° and 134°


Figure 2. Measuring thrust force and torque in the drilling process using Kistler 9272 dynamometer

2. Methodology

This study uses several stages of testing which are described in the following sub-sections.

2.1. Drilling Process

In this experiment, the input parameters are (1) the type of tool (HSS M2 and HSS M35), (2) points of angle (118 and 134 degrees), and (3) feeding speed (0.07 and 0.1 mm/s), and the output parameters to be studied are the thrust force and torque in the drilling process, measured using a Kistler 9272 dynamometer. The workpiece used in this study is an EMS 45 tool steel with a length of 200 mm, width of 20 mm, and thickness of 30 mm. The properties of the drilling tool can be seen in Table 11, and

the experimental process as well as the data collection procedure for the drilling process using the Kistler 9272 dynamometer can be seen in Fig. 2.

2.2. Finite Element Method

During a metal-cutting process, the workpiece material is subject to elastoplastic thermal deformation under high temperatures, considerable strain, and significant strain rate conditions. Therefore, a mathematical model needs to be constructed to measure the conditions and take appropriate actions accordingly. Johnson-Cook's mathematical model is commonly used to illustrate the effect of strain rate on the stress-strain curve in the machining process, as shown in the following formulation.

$$\sigma = [A + B(\epsilon)^n] \cdot [1 + C \ln \dot{\epsilon} / \dot{\epsilon}_0] \cdot \left[1 - \frac{(T - T_0)^m}{(T_m - T_0)} \right] \quad (1)$$

where σ is stress, A is yield strength, B is modulus of hardening, ϵ is plastic strain, n is hardening coefficient, C is strain rate sensitivity coefficient, $\dot{\epsilon}$ is strain rate, $\dot{\epsilon}_0$ is reference of plastic strain rate, T is temperature, T_m is melting temperature, T_0 is temperature of reference, and m is coefficient of thermal softening. The first part of this mathematical model describes the relationship between strain and stress, the second part describes the relationship between strain rate and stress, and the last part describes the relationship between stress value and material temperature during plastic deformation. Next, the Johnson-cook parameters for working material EMS-45 and tool steel can be seen in Table 2 and Table 3.

The theory of plasticity in metal formation is essential in determining plastic deformation in the drilling process. This deformation mechanism is used to determine the metal flow characteristics, final geometry of the product, and mechanical properties of the working piece after drilling.

For modeling material in a plastic state, the Johnson-Cook formulation requires a strain rate parameter. According to Chao (1951), the strain rate for the metal-cutting process is within the range of 103-106 s⁻¹. The value of strain rate in a machining process is influenced by cutting speed, initial thickness, and angle of thread inclination, which is formulated by the following Drucker [24] equation:

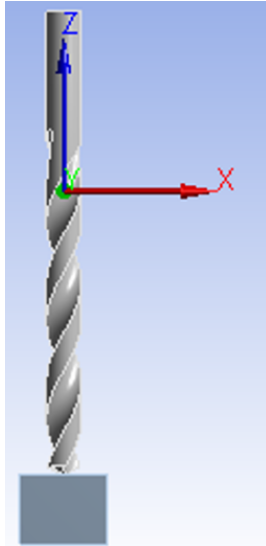
$$\dot{\epsilon}_{xy} = \frac{0, 2 \epsilon_{xy} v \sin \varphi}{h} \quad (2)$$

Table 2. Mechanical properties of working material and tool steels.

Parameter	Working Material(EMS-45) [20]	HSS M2 [21]	HSS M35 [21]
Density (ρ)	7800 kg/m ³	8100 kg/m ³	8000 kg/m ³
Thermal conductivity (K)	38 W/(m K)	24 W/(m K)	24 W/(m K)
Specific heat (c)	420 J/(kg K)	420 J/(kg K)	420 J/(kg K)
Modulus of elasticity	200 Gpa [22]	225 GPa	230 GPa
Thermal expansion ratio	$6.39 \times 10^{-6}/K$ [22]	$12.1 \times 10^{-6}/K$	$11.6 \times 10^{-6}/K$

Table 3. Johnson-Cook parameters for working material and tool steels.

Parameter	Working Material (EMS-45) [20]	Tool steel [23]
Yield strength (A)	553 MPa	391.3 MPa
Hardening modulus (B)	600 MPa	723.9 MPa
Coefficient of strain-rate sensitivity (C)	0.0134	0.1144
Coefficient of hardening (n)	0.234	0.3067
Coefficient of thermal softening (m)	1	0.9276

**Figure 3.** An illustration of a 3D modelling using FEM software

where $\dot{\epsilon}_{xy}$ is strain rate, ϵ_{xy} is shear strain, v is cutting speed, h is $t_1/20$, t_1 is initial chip thickness, and Φ is angle of thread inclination.

This research starts with determining the specifications and dimensions of the tool and workpiece. Next, 3D tools and workpieces are then designed using a 3D CAD software program. The 3D modeling design is tested using Ansys 2021 R2 software with initial setting parameters (FEM). ANSYS dynamic modeling is then employed for modeling since the drilling process occurs with high strain rates and temperatures. The workpiece is gripped at the bottom and modeled as a boundary fixed. The element type used is a tetrahedron because the shape of the tool is not symmetrical about the tool axis. The contact condition between the workpiece (slave) and the tool (master) is separation with friction. The FEM results are then compared with the experimental results to calculate the difference in error between the two methods. The setting parameter of FEM is then tuned using feedback error continuously until the error difference is less than 5%.

The modeling test is carried out by using different types of tools, namely HSS M2 and HSS M35. The feeding speed parameters are also varied (0.07 and 0.1 mm/rev), and the points of angle are varied, namely 118° and 134°. Further, the output parameters (thrust force and torque) are calculated based on the maximum compressive force

in the normal direction (z) as shown in Fig 3.

2.3. Experimental and FEM Result

The measurement results of thrust force and torque with various input parameters (tool types, point of angles, and feed rates) obtained using the experimental and FEM are shown in Table 4.

2.4. Backpropagation Neural Network (BPNN)

Backpropagation Neural Network (BPNN) is a supervised learning algorithm for modeling the relationship between parameter input and target in milling. BPNN consists of 3 layers, namely input, hidden, and output layers. All data is used to update the weight on the hidden layer through a series of processes (epochs). This is to minimize the mean squared error (MSE) between the target and output predicted by BPNN. The selected BPNN parameters in modeling the relationship between the input and target parameters can be seen in Table 5. These parameter values should be tuned to obtain minimum MSE, making prediction results of BPNN more accurate. The values of parameters no 1, 2, 5, and 8 are suggested by MATLAB. In contrast, the values of parameters 3, 4, 6, and 7 are determined by our experience.

Specifications of the best BPNN network can be detailed as follows: (1) the number of hidden layers is six layers, (2) the number of neurons in each hidden layer is eight neurons, (3) the activation function of the hidden layers is tansig, and (4) the Mean Squared Error (MSE) is 0.0047215. The best BPNN network topology with the minimum MSE value can be seen in Fig. 4. Next, the correlation coefficient value for training, validation, and testing can be seen in Fig. 5. Since the correlation coefficient value is close to 1, the relationship between the data in training, testing, and validation is said to be powerful.

3. Metaheuristic Method

This study uses two stages of the metaheuristic method, namely Genetic Algorithm (GA) and Simulated Annealing (SA). Those metaheuristics are described below.

3.1. Genetic Algorithm (GA)

Genetic algorithm is one of the optimization methods inspired by natural selection. This method looks for the optimal value through a series of processes, namely selection, crossover, and mutation. The procedure for using the GA method is explained as follows:

Table 4. Comparison of experimental vs FEM results in drilling

Tool types	Point of angles (degrees)	Feed rates (mm/rev)	Thrust force (N)	Torque (Nm)	Data Types
1	118	0.07	1678	3.391	Experimental
1	118	0.07	1603	3.471	Experimental
1	118	0.07	1588	3.3976	Experimental
1	118	0.07	1627.3	3.45	FEM
1	118	0.1	2656	4.082	Experimental
1	118	0.1	2566	4.095	Experimental
1	118	0.1	2846	4.18	Experimental
1	118	0.1	2623	4.38	FEM
1	134	0.07	2523	3.591	Experimental
1	134	0.07	2546	3.571	Experimental
1	134	0.07	2719	3.456	Experimental
1	134	0.07	2812	3.23	FEM
1	134	0.1	2675	4.182	Experimental
1	134	0.1	2746	3.995	Experimental
1	134	0.1	2887	3.876	Experimental
1	134	0.1	2927	3.85	FEM
2	118	0.07	1411	4.396	Experimental
2	118	0.07	1652	4.386	Experimental
2	118	0.07	1576	4.217	Experimental
2	118	0.07	1650	4.33	FEM
2	118	0.1	2143	3.974	Experimental
2	118	0.1	2174	3.753	Experimental
2	118	0.1	2245	3.725	Experimental
2	118	0.1	2106.7	3.85	FEM
2	134	0.07	1897	3.096	Experimental
2	134	0.07	2041	2.878	Experimental
2	134	0.07	1911	2.924	Experimental
2	134	0.07	2067.2	2.81	FEM
2	134	0.1	2489	3.591	Experimental
2	134	0.1	2478	3.571	Experimental
2	134	0.1	2357	3.85	Experimental
2	134	0.1	2592.4	3.56	FEM

Table 5. BPNN tuning parameters

No	Parameter	Values
1	Ratio data for training, testing and validation	70%:15%:15%
2	Variation of activation function	Harlim, Hardlims, Satlin, logsig, tansig, and purelin
3	Number of hidden layers	1:10 layers
4	Number of nodes each hidden layer	1:10 nodes
5	Stopping criterion	Max epoch (10000 epochs)
6	Parameter for selecting best BPNN network	Mean Squared Error (MSE)
7	Learning rate	0.001
8	Training algorithm	Levenberg-Marquardt

Table 6. Specification of backpropagation neural network (BPNN)

Items	Value
Number of chromosomes	100
Composition of chromosomes;	
Variable X (bits)	12
Variable Y (bits)	11
Stopping criteria: number of generations	10000
cross-over methods	uniform cross-over
Selection Method	Roulette wheel

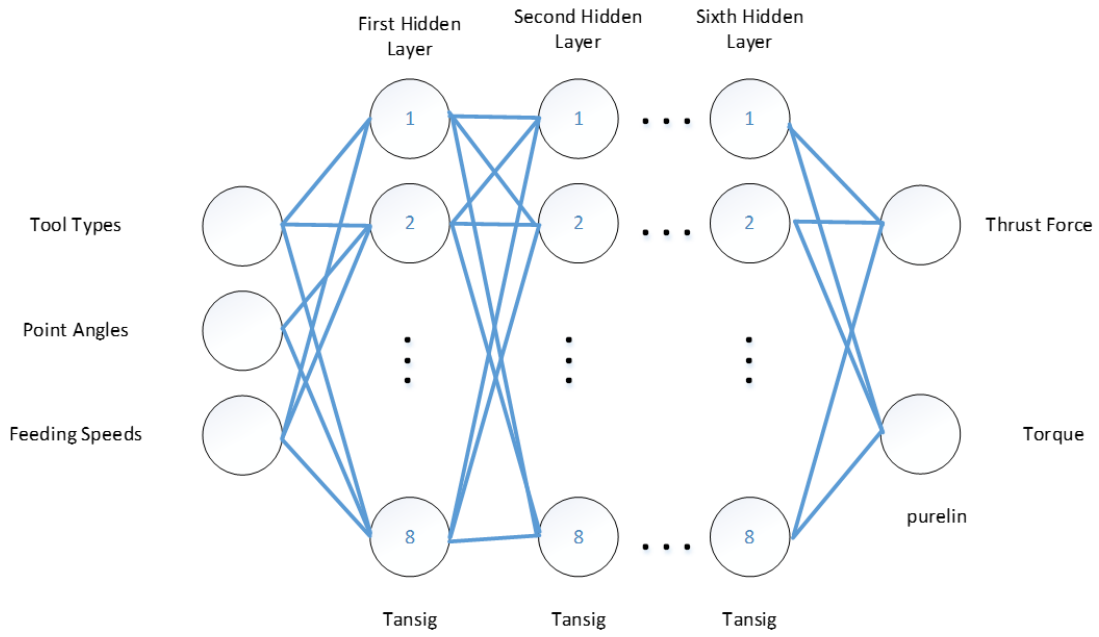


Figure 4. The best BPNN's network topology

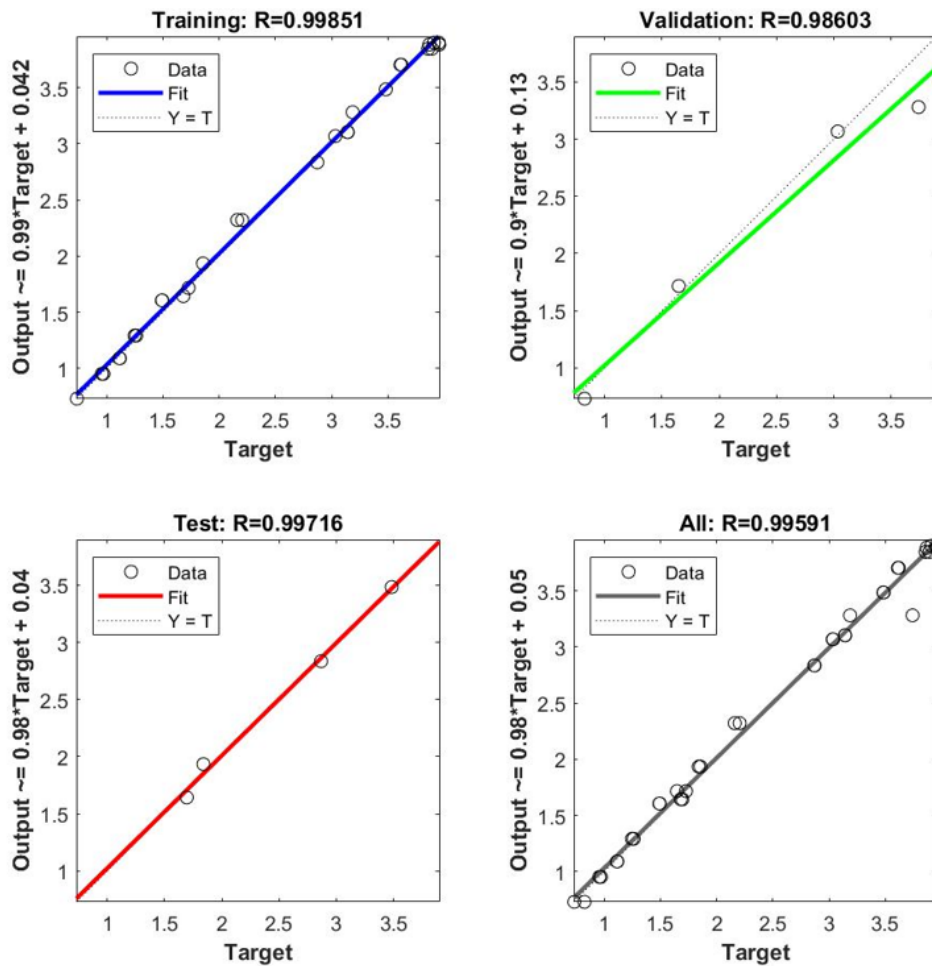


Figure 5. Correlation coefficient of the best BPNN's network

1. Randomly generating the initial population,
2. Calculating the fitness value of each individual in the population,
3. Using the fitness value for selecting elites,
4. Performing crossover between two elites to produce offsprings,
5. Randomly conducting the mutation process for several individual's cells, and
6. If the best individual fitness value has not met the stopping criteria, the series of processes from number 1-6 is to be repeated.

The GA parameters used to identify the optimal solution can be seen in Table 6.

3.2. Simulated Annealing (SA)

Simulated annealing (SA) is an optimization method that is completed based on the annealing process. Annealing is the process of heating metal/alloy at a specific temperature and cooling it at room temperature to increase the ductility and reduce the metal's brittleness. In the beginning, an initial solution is selected, which represents the conditions of the material before the process starts. The free movement of the atoms in the material is represented in the modifications to the initial/temporary solution. When the temperature parameter (T) is set high, the existing temporary solution can be freely modified. Furthermore, when the temperature is gradually reduced in the next stage, the possibility of accepting a modification decreases so that the freedom rate to modify the solution gets narrower until the optimal solution is obtained. In general, the SA procedure for achieving the optimum value can be explained as follows:

1. Choose an initial solution (S_0), initial temperature (T_0), final temperature (T_f) and number of iteration (n_{iter})
2. Determine cooling schedule which is formulated by the following equation (Kirkpatrick, 1983).

$$T_{(k)} = T_o \times \exp\left(\frac{-c}{k}\right) \quad (3)$$

where:

- c = 0.1
 k = 1
 Number of iterations = 100 each temperature drop

3. While $T_f < T_0$ or iteration $< n_{iter}$ do
 - a. Select solution (S), where $S \in N(S_0)$
 - b. Calculating the objective function difference (δ), where:

$$\delta = f(S) - f(S_0) \quad (4)$$

- c. If $\delta < 0$
 $S_0 = S$
 else
 generate random value (r), $r \sim U(0,1)$
 If $r < \exp\left(\frac{-\delta}{\tau}\right)$, then $S_0 = S$
 end

d. Define $t = T(k)$

4. Return S_0

4. Result and Discussion

Fig 6(a) describes that higher torque can be achieved by selecting tool type 1, point of angle at 118° , and feed rate at 0.1 mm/rev. Fig 6b shows the higher thrust conducted by tool type 1, point of angle at 134 degrees, and feed rate at 0.1 mm/rev. This phenomenon indicates that tool type HSS M2 and lower feed rate significantly affect greater torque and thrust in drilling. Soepangkat et al. [15] concluded that the value of thrust and torque increase by increasing feeding speed. Increasing feeding speed means increasing the volume of material to be removed, and the drilling tool needs extra effort/thrust force to perform it [22, 23]. Furthermore, Fig 6(b) also depicts that increasing the point of angle increases the thrust value. Increasing the angle point of the drilling tool decreases the cutting edge's length, decreases the support at the circumstance, and reduces the trust force [23].

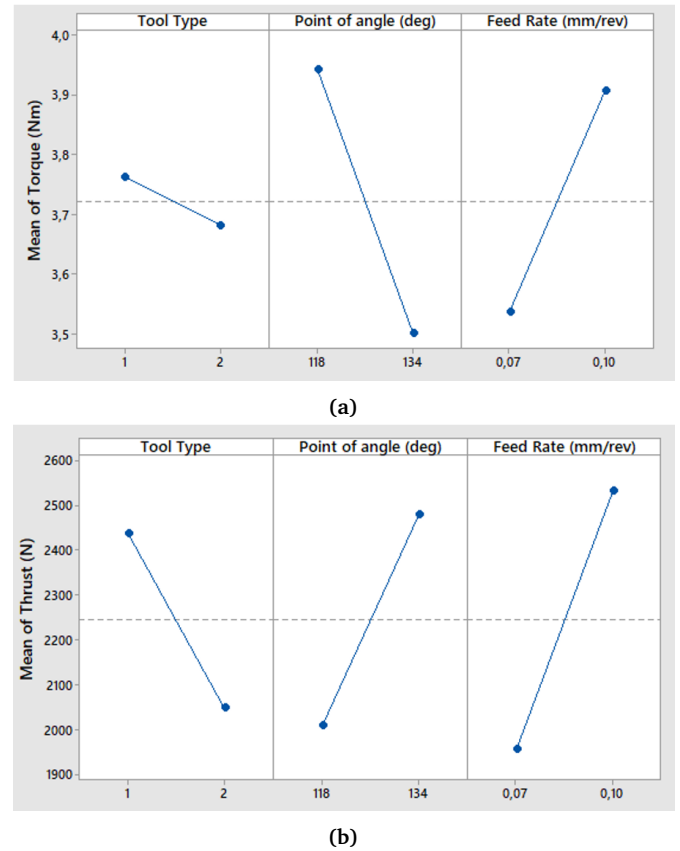


Figure 6. Effect of drilling process: a. Torque, b. Thrust

Table 7. Generated five optimum candidates by genetic algorithm (GA)

Type of drill tool	Drilling parameter inputs		Drilling parameter output	
	point of angle (degree)	feeding speed (mm/rev)	Thrust force (N)	Torque (Nm)
1.380	118.815	0.098	1.616.269	3.024
1.066	132.054	0.1	1.615.714	3.024
1.090	131.929	0.099	1.616.196	3.024
1.023	132.180	0.099	1.615.821	3.024
1.376	119.882	0.098	1.616.623	3.025

Table 8. Multi-objective optimization result using simulated annealing (SA)

Type of drill tool	Drilling parameter inputs		Drilling parameter output	
	point of angle (degree)	feeding speed (mm/rev)	Thrust force (N)	Torque (Nm)
1.1	133.4	0.09	1.615.162	3.023

Table 9. Modified Simulated Annealing Results

Type of drill tool	Drilling parameter inputs		Drilling parameter output	
	point of angle (degree)	feeding speed (mm/rev)	Thrust force (N)	Torque (Nm)
1 (HSS-M2)	132.28	0.1	1615.2	30.236

Table 10. Comparison between SA prediction and confirmation experiment

Type of drill tool	Drilling parameter inputs		Thrust force (N)		Torque (Nm)	
	point of angle (degree)	feeding speed (mm/rev)	Pred/Exp	error	Torque (Nm)	error
1 (HSS-M2)	132.28	0.1	1615.2/1705	5.6%	3.0236/3.16	4.5%

GA was applied as the initial method in the multi-objective optimization for conducting a global search and producing five candidates, as shown in Table 7. SA is then utilized for performing a local search and increasing the accuracy of GA. In the first iteration, the best candidate generated by GA is then employed as an initial candidate by SA. At the end of the iteration, SA chooses the tool-type = 1.02 as the optimal solution, as shown in Table 8.

Next, because the type of drilling tool used in the drilling process is 1 (HSS-M2), then the optimization value must be changed. This process is carried out by redefining the fitness function equation using the dynamic penalty formulation shown below:

$$fitness(x) = f(x) + (C \times t)^\alpha \sum_{j=1}^m \varphi_j^\beta(x) \quad (5)$$

Where $f(x)$ is an original fitness value, C, α and β are constants defined by 0.5, 2 and 2. $\varphi_j(x)$ is a violation function with constrain j , with m as the number of constraints, and t is generation. The dynamic penalty formulation has been implemented to reduce the original fitness value when the violation value is not equal to zero using predetermined parameters. The result of redefining the optimization value due to the limitation of the

tool type can be described as follows: (1) the type tool is HSS-M2, (2) the point of angle is 132.28° , (3) the feeding speed is 0.1 mm/s, (4) thrust force is 1615.2 N, (5) torque is 3.0236 N.m., as shown in Table 9.

The confirmation experiment is then performed using the optimum drilling parameter setting. It is repeated five times, and the mean value can be seen in Table 10. Based on this table, the error value between the BPNN-GA-SA prediction results and confirmation experiment is below 6% for all the outputs. This validates that the predicted drilling parameter output has an insignificant difference from the experimental data.

5. Conclusion

In this study, the FEM is used to reproduce data for the drilling process. Increasing the data leads to the increasing performance of the BPNN's network model. The GA and SA methods are later used to identify the most optimal value in drilling by utilizing the network model. From the experimental work and optimization, the following concluding remarks are drawn:

1. Researchers can use FEM to simulate the drilling process so that large amounts of data can be obtained at low cost.
2. BPNN can be used to predict the correlation between

drilling input parameters (type of drill tools, points of angle, and feeding speed rates) and output parameters (thrust force and torque). The best network obtained is with 3-8-8-8-8-8-2 architecture, comprising three neurons of an input layer, six hidden layers with eight neurons, and an output layer with two neurons. The type of activation function used is tansig with the mean squared error (MSE) of 0.0047215.

3. The genetic algorithm (GA) method can effectively be used to set the initial predictions. Furthermore, the results from the GA are used by the simulated annealing (SA) method to precisely predict the optimum value.

References

- [1] R. Hambli, "Blanking tool wear modeling using the finite element method," *International Journal of Machine Tools and Manufacture*, vol. 41, no. 12, pp. 1815–1829, 2001.
- [2] K. Park, C. J. VanTyne, and Y. Moon, "Process analysis of multistage forging by using finite element method," *Journal of Materials Processing Technology*, vol. 187, pp. 586–590, 2007.
- [3] R. Quiza, O. López-Armas, J. P. Davim, R. Quiza, O. López-Armas, and J. P. Davim, "Finite element in manufacturing processes," *Hybrid Modeling and Optimization of Manufacturing: Combining Artificial Intelligence and Finite Element Method*, pp. 13–37, 2012.
- [4] I. Singh, N. Bhatnagar, and P. Viswanath, "Drilling of uni-directional glass fiber reinforced plastics: Experimental and finite element study," *Materials & Design*, vol. 29, no. 2, pp. 546–553, 2008.
- [5] J. Strenkowski, C. Hsieh, and A. Shih, "An analytical finite element technique for predicting thrust force and torque in drilling," *International Journal of Machine Tools and Manufacture*, vol. 44, no. 12-13, pp. 1413–1421, 2004.
- [6] O. Isbilir and E. Ghassemieh, "Finite element analysis of drilling of carbon fibre reinforced composites," *Applied Composite Materials*, vol. 19, pp. 637–656, 2012.
- [7] O. Isbilir and E. Ghassemieh, "Finite element analysis of drilling of titanium alloy," *Procedia engineering*, vol. 10, pp. 1877–1882, 2011.
- [8] W. A. Lughmani, K. Bouazza-Marouf, and I. Ashcroft, "Drilling in cortical bone: a finite element model and experimental investigations," *Journal of the mechanical behavior of biomedical materials*, vol. 42, pp. 32–42, 2015.
4. The combination of BPNN-GA-SA can be used as a recommendation to design an angle point for the drilling tool and determine the optimum feeding speed in drilling. The optimum input-output parameter value in drilling for material EMS-45 can be explained with the following specifications: (a) type of drill tool = HSS-M2, (b) point of angle = 132.28°, (c) feeding speed = 0.1 mm/s, (d) thrust force = 1615.2 N, and (e) torque = 3.0236 Nm.
5. Since the error value between the BPNN-GA-SA prediction results and confirmation experiment is below 6%, it was concluded the prediction output has an insignificant difference from the experimental data.
- [9] V. A. Phadnis, F. Makhadmeh, A. Roy, and V. V. Silberschmidt, "Drilling in carbon/epoxy composites: Experimental investigations and finite element implementation," *Composites Part A: Applied Science and Manufacturing*, vol. 47, pp. 41–51, 2013.
- [10] F. P. Nurullah, B. Pramujati, S. Suhardjono, M. K. Effendi, B. O. P. Soepangkat, and R. Norcahyo, "Multi response prediction of end-milling cfrp with back-propagation neural network," in *AIP Conference Proceedings*, vol. 2114, AIP Publishing, 2019.
- [11] D. E. Ighravwe and S. A. Oke, "Machining performance analysis in end milling: predicting using ann and a comparative optimisation study of ann/bb-bc and ann/pso," *Engineering Journal*, vol. 19, no. 5, pp. 121–137, 2015.
- [12] S. Panda, A. K. Singh, D. Chakraborty, and S. Pal, "Drill wear monitoring using back propagation neural network," *Journal of Materials Processing Technology*, vol. 172, no. 2, pp. 283–290, 2006.
- [13] A. Singh, S. Panda, D. Chakraborty, and S. Pal, "Predicting drill wear using an artificial neural network," *The International Journal of Advanced Manufacturing Technology*, vol. 28, pp. 456–462, 2006.
- [14] S. S. Panda, D. Chakraborty, and S. K. Pal, "Flank wear prediction in drilling using back propagation neural network and radial basis function network," *Applied soft computing*, vol. 8, no. 2, pp. 858–871, 2008.
- [15] B. O. P. Soepangkat, R. Norcahyo, M. K. Effendi, and B. Pramujati, "Multi-response optimization of carbon fiber reinforced polymer (cfrp) drilling using back propagation neural network-particle swarm optimization (bpnn-pso)," *Engineering Science and Technology, an International Journal*, vol. 23, no. 3, pp. 700–713, 2020.
- [16] V. Sonkar, K. Abhishek, S. Datta, and S. S. Mahapatra, "Multi-objective optimization in drilling of gfrp

- composites: a degree of similarity approach,” *Procedia Materials Science*, vol. 6, pp. 538–543, 2014.
- [17] K. Gallagher and M. Sambridge, “Genetic algorithms: a powerful tool for large-scale nonlinear optimization problems,” *Computers & Geosciences*, vol. 20, no. 7-8, pp. 1229–1236, 1994.
- [18] A. F. Shapiro, “The merging of neural networks, fuzzy logic, and genetic algorithms,” *Insurance: Mathematics and Economics*, vol. 31, no. 1, pp. 115–131, 2002.
- [19] R. L. Haupt, “An introduction to genetic algorithms for electromagnetics,” *IEEE Antennas and Propagation Magazine*, vol. 37, no. 2, pp. 7–15, 1995.
- [20] Y. Lin, Z. Bian, and X. Liu, “Developing a dynamic neighborhood structure for an adaptive hybrid simulated annealing–tabu search algorithm to solve the symmetrical traveling salesman problem,” *Applied Soft Computing*, vol. 49, pp. 937–952, 2016.
- [21] X.-H. Wang and J.-J. Li, “Hybrid particle swarm optimization with simulated annealing,” in *Proceedings of 2004 International Conference on Machine Learning and Cybernetics (IEEE Cat. No. 04EX826)*, vol. 4, pp. 2402–2405, IEEE, 2004.
- [22] D. Drucker, “An analysis of the mechanics of metal cutting,” *Journal of Applied Physics*, vol. 20, no. 11, pp. 1013–1021, 1949.
- [23] B. McClain, S. A. Batzer, and G. I. Maldonado, “A numeric investigation of the rake face stress distribution in orthogonal machining,” *Journal of Materials Processing Technology*, vol. 123, no. 1, pp. 114–119, 2002.